Proceedings of 2004 IEEE/RSJ International Conference on Intelligent Robots and Systems
September 28 - October 2, 2004, Sendai, Japan

Contact Impedance Estimation for Robotic Systems

N. Diolaiti[1], C. Melchiorri[1], S. Stramigioli[2]

[1]DEIS, University of Bologna
Via Risorgimento 2, 40136 Bologna, Italy
{ndiolaiti,cmelchiorri}@deis.unibo.it

[2]CTIT & Drebbel Institute, Univ. of Twente
P.O. Box 217, 7500 AE Enschede, NL
S.Stramigioli@ieee.org

Abstract—**In this paper, the problem of the on-line estimation of the mechanical impedance during the contact of a robotic system with an unknown environment is considered. Indeed, the knowledge of the mechanical properties could allow to improve the interaction between robotic devices and unstructured and unknown environments, e.g. in telemanipulation tasks. A single-point contact is considered and the (nonlinear) Hunt-Crossley model is taken into account and its better physical consistency in describing the behavior of soft materials is discussed in comparison with the classical (linear) Kelvin-Voigt model. Finally, the on-line estimation algorithm is described and experimental results presented.**

I. Introduction

Interaction with unstructured and potentially unknown environments is one of the most challenging topics in robotics. Indeed, several problems affecting stability and performances arise when the motion of a robotic device is constrained. On the other side, the availability of an accurate description of mechanical properties of the environment could help to handle these problems in a more effective way, allowing to adapt robot controllers to current working conditions. In particular, these aspects have been pointed out in [1], where stability of impedance control [2] has been improved by means of an on-line estimation of contact stiffness and damping. These concepts have been also considered in [3], where different estimation algorithms are presented and discussed with particular attention to the on-line simulation of contact dynamics in space operations. Another field of application of such algorithms are master/slave bilateral teleoperation systems, by means of which human operators interact with remote environments. It is known [4] that the fidelity of force feedback, usually defined transparency, is affected by controllers and time delays in data transmission. This sensation is important e.g. in surgical applications, where the surgeon should be able to recognize human tissues by touching them and identifying their mechanical properties. Therefore, an on-line estimation of mechanical properties of *soft* tissues can be used to (partially) recover transparency and telepresence sensation, as suggested in [5] and in [6], thus making force feedback surgical systems more effective.

The first step towards the implementation of the on-line estimation of the impedance of objects interacting with a robotic device, is the choice of suitable contact models [7], able to describe contact dynamics (i.e. the relation between contact force and the compenetration of contacting bodies). Focusing on one-dimensional contacts, in this paper it is shown that the linear model, known also as *Kelvin-Voigt model*, commonly used to describe the interaction with stiff environments cannot be applied to soft materials, where viscous effects are relevant. On the other side, Hunt and Crossley [8] showed that it is possible to obtain a more physically consistent behavior [9] if the damping coefficient is made dependent on the bodies penetration. This contact model has been chosen to describe contact with compliant objects and an on-line estimation algorithm is presented here to identify characteristics parameters of different materials. Finally, the physical consistency of the model can be preserved by a proper generalization to the full geometrical contact description (6 dof), as discussed in [10].

This paper is organized as follows: Sect. II provides a brief overview on contact models, discussing in particular drawbacks affecting the linear contact model and the properties of the Hunt-Crossley model. Then, in Sect. III an on-line recursive algorithm for the parameters of the Hunt-Crossley model is presented. This algorithm has been applied to different materials in order to provide experimental confirmation (Sect. IV) to the theoretical considerations. Finally, conclusions and future work-plan are discussed in Sect. V.

II. Compliant contact models

The dynamics of contact is a complex event depending on many properties of contacting bodies, such as material, geometry, and velocity. Contact models such as the Kelvin-Voigt [11] linear model and the Hunt-Crossley [8] nonlinear model provide a time continuous description that relates the bodies penetration and the consequent reaction force. Therefore, parameters characterizing these models can be used to describe the interaction dynamics between a robotic device and surrounding objects. However, the following discussion points out that, despite its simplicity, the Kelvin-Voigt model is not consistent with the notion of coefficient of restitution, commonly used to characterize energy losses during impacts. The nonlinear model proposed by Hunt and Crossley, on the contrary, solves these drawbacks while retaining a certain computational simplicity.

A. *Coefficient of restitution*

The contact process can be divided into two main phases: the phase starting with the contact at time $t = 0$ and ending at time $t = t_M$, corresponding to the maximum deformation x_M, is called *compression*, and is followed by the *restitution* phase, taking place from $t = t_M$ to the instant t_F when bodies separate [12], [7]. Because of energy dissipation, the total kinetic energy of colliding bodies diminishes after impact and the coefficient of restitution e, empirically determined for several materials, is widely used to characterize energy loss due to impacts. According to the Newton model [7], e relates the relative velocity of bodies along normal direction after impact (v_o) to the initial relative velocity (v_i):

$$v_0 = -ev_i \tag{1}$$

The coefficient of restitution is the unity only in perfectly reversible impacts, where energy is completely conserved. For low impact velocities within the elastic range of materials, experiments [12] showed that e depends on the initial velocity v_i and that, with reasonable accuracy, the following relation holds:

$$e = 1 - \alpha v_i \tag{2}$$

where α, usually between 0.08 and 0.32 sec/m, depends on the materials of colliding bodies. According to (2), energy dissipated ΔH during impact by a point mass m whose initial momentum is $p_i = mv_i$ can be expressed as:

$$\Delta H = \frac{p_i^2}{2m}(1 - e^2) = \frac{p_i^2}{2m}\left[1 - (1 - \alpha v_i)^2\right] \tag{3}$$

Since the quadratic term $\alpha^2 v_i^2$ is relatively small, the following approximation is usually considered:

$$\Delta H \simeq \alpha v_i \frac{p_i^2}{m} \tag{4}$$

B. Linear contact model

The coefficient of restitution is therefore an accurate way to experimentally characterize impacts and summarizes energy dissipation due to complex phenomena such as wave propagation, plasticity, friction and heat. However, in most applications also information about contact force and dynamics are needed and the simplest way to describe the mechanical impedance of an object is the linear Kelvin-Voigt [11] contact model. It can be obtained considering that an ideal visco-elastic material is represented by the mechanical parallel of a linear spring and a damper. The force F exerted by the material on a probe during contact is expressed by:

$$F(t) = \begin{cases} Kx(t) + B\dot{x}(t) & x \geq 0 \\ 0 & x < 0 \end{cases} \tag{5}$$

where $\dot{x}$ is the penetration velocity of the probe and K and B are the elastic and viscous parameters of the contact. The hysteresis loop obtained simulating impact of mass m with a material modeled by (5) is shown in Fig. 1(a); the compression phase corresponds to the arc connecting point A to the maximum penetration x_M, while the lower arc represents the restitution phase. Physical inconsistencies of (5) are related to the unnatural shock forces at the moment of impact (point A) and to the tensile or "sticky" forces at the moment of load removal (point B).

Moreover, the dissipated energy ΔH is represented by the area enclosed by the hysteresis loop and can be computed as the algebraic sum of the energies H_1, H_2, H_3. These energies are also plotted in Fig. 1(b), showing power flow $P(t) = F(t)\dot{x}(t)$.

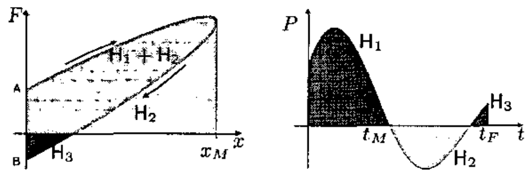

(a) Hysteresis loop (b) Power exchange

Fig. 1. Behavior of a material described by the Kelvin-Voigt model (pictures are in different scales)

Since positive areas represent energy flowing from the mass to the touched material and vice-versa, H_3 represents power that is extracted from the mass even in the restitution phase, where $\dot{x}(t) < 0$, and this is in contrast with experiments.

These physical inconsistencies happen because, when the penetration is small, the force F in (5) mainly depends on the damping term, that is not related to x. As well discussed in [8], [9] and [7], the energetic deviation from the correct behavior is summarized by the fact that the coefficient of restitution obtained from (5) does not depend on the impact velocity, in contrast with (2).

C. The Hunt-Crossley model

These problems can be overcome if the viscous force is made dependent on the penetration depth, as first proposed by Hunt and Crossley [8]:

$$F(t) = \begin{cases} kx^n(t) + \lambda x^n(t)\dot{x}(t) & x \geq 0 \\ 0 & x < 0 \end{cases} \tag{6}$$

where the exponent n is a real number usually close to the unity, that takes into account the geometry of contact surfaces. Notice that when $n = 3/2$ the elastic term of (6) exactly matches the force resulting from the Hertzian theory for spheres contacting in static conditions [13]. The new hysteresis loop, Fig. 2(a), shows that (6) produces a behavior that is more consistent with experimental observations.

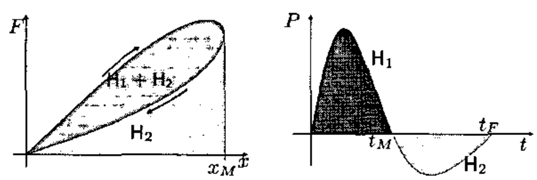

(a) Hysteresis loop (b) Power exchange

Fig. 2. Behavior of a material described by the Hunt-Crossley model (pictures are in different scales)

Moreover, as shown in [8] and more formally in [9], for low impact velocities v_i (6) is consistent with (2). Indeed, the energy balance equation during impact with a material whose impedance is described by (6) is:

$$\frac{p_i^2}{2m} = \frac{p^2(t)}{2m} + H_k(t) + H_\lambda(t) \tag{7}$$

where $p_i = mv_i$ is the initial momentum, $H_k(t)$ is the stored elastic energy and $H_\lambda(t)$ represents the energy dissipated because of the damping term:

$$H_k(t) = \int_0^t kx^n(\tau)\dot{x}(\tau)d\tau \tag{8}$$

$$H_\lambda(t) = \int_0^t [\lambda x^n(\tau)\dot{x}(\tau)]\dot{x}(\tau)d\tau \tag{9}$$

For perfectly elastic materials ($\lambda = 0$), the hysteresis loop degenerates to a line and it is possible to relate initial kinetic energy with the maximum penetration $x_{M,k}$:

$$v_i^2 = \frac{2k}{m}\frac{x_{M,k}^{n+1}}{n+1} \tag{10}$$

and finally a relation between penetration x and velocity $\dot{x}$ is found:

$$\dot{x}(t) = \sqrt{\frac{2k}{m(n+1)}}\sqrt{x_{M,k}^{n+1} - x^{n+1}(t)} \tag{11}$$

This expression can be considered valid ($x_M \simeq x_{M,k}$), with a certain degree of approximation, also for materials with small damping coefficient and allows to write:

$$\Delta H = H_\lambda(t_F) = \int_0^{t_F} \lambda x(\tau)^n \dot{x}(\tau)^2 d\tau \simeq 2\int_0^{x_M} \lambda x^n \dot{x} dx \tag{12}$$

Finally, the comparison of the expressions of ΔH obtained by substituting (11) into (12) and into (4), allows to relate the coefficients of the Hunt-Crossley model to the coefficient of restitution of a given material:

$$\lambda = \frac{3}{2}\alpha k \tag{13}$$

Note that the dependence of the coefficient of restitution e on impact velocity v_i is thus recovered, thus obtaining consistent results from the energetic point of view.

III. Estimation Algorithm

Because of its simplicity and its advantages with respect to the linear model, the Hunt-Crossley model has been chosen to represent impact dynamics.

A linear regression algorithm can be implemented if force, position and velocity measures are available. Since (6) is non linear with respect to the exponent n, the main idea is to separate the estimation of k and λ from the estimation of n. In this way, we can write two recursive least-squares estimators Γ_1 and Γ_2 [14] interconnected via feedback, as shown in Fig. 3.

In particular, Γ_1 estimates k and λ minimizing the cost function $V_N(k, \lambda)$ defined as follows:

$$V_N(k,\lambda) := \frac{1}{N}\sum_{h=1}^{N}\varepsilon_1^2(h) \tag{14}$$

$$\varepsilon_1(h) := F(h) - [k + \lambda\dot{x}(h)]x^n(h) \tag{15}$$

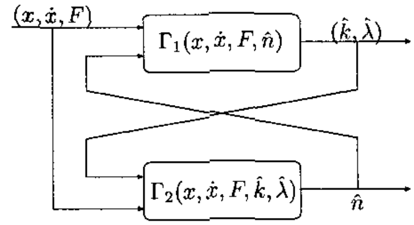

Fig. 3. On-line parameters estimator for the Hunt-Crossley model

where $h = 0, 1, 2, \ldots$ represents the discrete time variable ($t = hT$, being T the sample time), and N is the number of measures acquired from the beginning of the estimation process. It is here considered, that $\langle\varepsilon_1\rangle$, summarizing model errors and measurement noise, is a zero mean stochastic process. Let $\hat{\theta}_1(h) = [\hat{k}(h), \hat{\lambda}(h)]^T$ be the vector of estimates at time $t = hT$, $\mu_1 = [x^n(h+1), x^n(h+1)\dot{x}(h+1)]^T$ the vector of input signals and $\varphi_1(h) = F(h)$ the system output; the estimator Γ_1 is implemented by the following recursive equations [14]:

$$\begin{aligned}
\hat{\theta}_1(h+1) &= \hat{\theta}_1(h) + Q_1(h+1)\left[\varphi_1(h+1) - \mu_1^T\hat{\theta}_1(h)\right] \\
Q_1(h+1) &= R_1(h)\mu_1\left[\beta + \mu_1^T R_1(h)\mu_1\right]^{-1} \\
R_1(h+1) &= \tfrac{1}{\beta}\left[\mathbb{I} - Q_1(h+1)\right]R_1(h)
\end{aligned} \tag{16}$$

where β represents the forgetting factor limiting the estimation to more recent measures.

On the other side, an expression of (15) that is linear with respect to the parameter n can be obtained by means of algebraic manipulation:

$$\log\varepsilon_2(h) = \log\frac{F(h)}{k + \lambda\dot{x}(h)} - n\log x(h) \tag{17}$$

with

$$\varepsilon_2(h) := 1 + \frac{\varepsilon_1(h)}{[k + \lambda\dot{x}(h)]x^n(h)} \tag{18}$$

If ε_1 is small with respect to the force computed according to the Hunt-Crossley model (6), it is possible to write the following series expansion of (17):

$$\log\varepsilon_2 = \log\left(1 + \frac{\varepsilon_1}{[k+\lambda\dot{x}]x^n}\right) \simeq \frac{\varepsilon_1}{[k+\lambda\dot{x}]x^n} \tag{19}$$

Therefore, if the previous assumption holds and $\langle\varepsilon_1\rangle$ is independent on the force computed according to (6), $\langle\log(\varepsilon_2)\rangle$ can be considered as a stochastic process with zero mean and it is possible to estimate n by means of a recursive least-square procedure minimizing the cost function $W_N(n)$:

$$W_N(n) := \frac{1}{N}\sum_{h=1}^{N}\log^2(\varepsilon_2(h)) \tag{20}$$

Finally, Γ_2 is implemented by means of equations analogous to (16), with $\hat{\theta}_2(h) = \hat{n}(h)$, $\mu_2 = \log x(h+1)$ and $\varphi_2(h) = \log(F(h)/(k + \lambda\dot{x}))$.

With respect to Kalman filtering techniques [15], the proposed algorithm does not require to perform local linearizations of the process equation (6) and, by taking advantage of the particular structure of the Hunt-Crossley, handles the nonlinearity by means of the interconnection of two linear estimators.

However, because of this interconnection, the value of n used by Γ_1 as well as the value of these parameters used by Γ_2 is not the "true" value but the estimated one. For this reason, beside measurement noise and model error, each estimator behaves as an additional source of noise that could compromise the convergence of the algorithm. These considerations lead to rewrite estimation errors (15) and (17) as:

$$\varepsilon_1'(h) = F(h) - (k + \lambda \dot{x}(h))\, x^{\hat{n}}(h) \tag{21}$$

$$\log \varepsilon_2'(h) = \log \frac{F(h)}{\hat{k} + \hat{\lambda}\dot{x}(h)} - n \log x(h) \tag{22}$$

where the effect introduced by the use of estimates instead of true parameters values is considered. Therefore, provided that elementary estimators would converge, the convergence of their feedback interconnection is obtained if additional disturbances do not bias the stochastic processes $\langle \varepsilon_1' \rangle$, $\langle \log(\varepsilon_2') \rangle$ expressing residuals between measured and estimated forces for $(\hat{k}, \hat{\lambda})$ and $\hat{n}$ respectively.

The relation between ε_2 and ε_2' is given by:

$$\log \varepsilon_2'(h) \; = \; \log \varepsilon_2(h) - \log \left(1 + \frac{\delta k + \delta \lambda x(\dot{h})}{k + \lambda x(\dot{h})} \right) \tag{23}$$

where $\delta k = \hat{k} - k$ and $\delta \lambda = \hat{\lambda} - \lambda$ are the estimation errors. By computing its series expansion, recalling (19), we obtain:

$$\log \varepsilon_2' \simeq \log \varepsilon_2 - \frac{\delta k + \delta \lambda \dot{x}}{k + \lambda \dot{x}} \simeq \frac{\varepsilon_1 - x^n(\delta k + \delta \lambda \dot{x})}{x^n (k + \lambda \dot{x})} \tag{24}$$

Hence, the additional noise due to feedback interconnection has to be dominated by $\varepsilon_1(h)$ so that $\langle \log(\varepsilon_2') \rangle$ is still a zero mean process:

$$\|\delta k + \delta \lambda \dot{x}\| \ll \left\| \frac{\varepsilon_1}{x^n} \right\| \tag{25}$$

At the beginning of the estimation process, when the estimation errors δk and $\delta \lambda$ can be considerable, the penetration x is small and therefore this condition is satisfied. Therefore, the use of $(\hat{k}, \hat{\lambda})$ within the Γ_2 estimator does not alter its convergence properties and the overall feedback estimator provides unbiased estimates $\hat{k}$, $\hat{\lambda}$, $\hat{n}$ of parameters of (6). Moreover, the impact of initial estimates on the convergence of the algorithm is reduced by the use of a forgetting factor, that allows to identify modifications in touched materials by limiting the estimation only to the most recently acquired measures.

IV. Experimental results

In order to experimentally verify the above estimation algorithm, a laboratory setup has been implemented. The setup consists of a linear electric motor equipped with a position sensor and a load cell, Fig. 4.

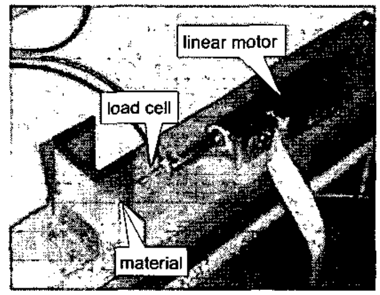

Fig. 4. Experimental setup.

The measures required by the estimation algorithm have been obtained by imposing a motion profile to a linear motor touching different materials. The contact force F is measured by means of the load cell, the penetration x is measured by comparing the current motor position with the position measured at the time of impact, and finally the penetration velocity $\dot{x}$, that has been kept limited in order to achieve a stable contact, is obtained from x by means of a state variable filter. The linear motor and the load cell are interfaced to a standard PC running control and estimation algorithms in a mixed MATLAB/RTLinux environment. In the experimental activity, the sampling time has been set to $T = 1$ msec. Several materials have been used and here, in particular, the results obtained with a thin layer of plastic material, characterized by a stiff behavior, and a soft gel, whose energy dissipation is relevant, are described.

A. Choice of motion profile for probe device

Performances of recursive estimation are influenced mainly by two factors: the correctness of the Hunt-Crossley model in describing the behavior of compliant material and the trajectory followed by the probe device, that should provide a sufficient level of excitation to the system.

It is possible to evaluate both these aspects from a graphical point of view. Indeed, parameters for a certain vector of measures $[x(h), \dot{x}(h), F(h)]$ acquired at time $t = hT$, lie on the null manifold described by the equation:

$$F(h) - kx^n(h) - \lambda x^n(h)\dot{x}(h) = 0 \tag{26}$$

In the ideal case, the Hunt-Crossley model perfectly de-

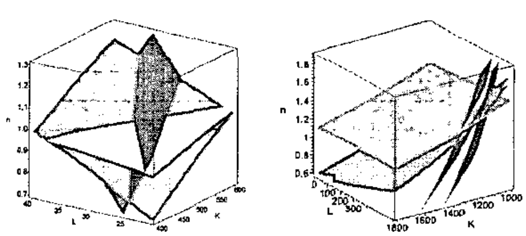

(a) Ideal case (b) Experimental data

Fig. 5. Intersections of null surfaces in ideal and real case

scribes contact dynamics and surfaces related to measures acquired throughout the identification process intersect exaactly in a point of the space of parameters (k, λ, n). This situation is shown in Fig. 5(a), where the point $k = 500$, $\lambda = 30$, $n = 1.1$ identifies the parameters of a simulated material. In a real case, where model errors and measure noise are present, surfaces intersections belong to a bounded subset of the parameters space, e.g. shown in Fig. 5(b), where a subset approximately centered on $k = 1100$, $\lambda = 40$, $n = 1.2$ is determined.

Since the application of the estimation algorithm has to be independent on the trajectory of the robotic systems, a sinusoidal trajectory has been considered. This kind of trajectory represents the lowest level of excitation that can be provided to the estimator, while the nonlinearity of (6) spreads the sinusoidal input over a wider frequency range thus enabling the algorithm to discriminate between equivalent solutions, as illustrated in Fig. 5(b).

B. Stiff material

Esperimental results related to the thin layer of plastic materials are presented in Fig. 6 and in Fig. 7. In particular, the hysteresis loop reported in Fig. 6(a) shows that energy dissipation is low and the behavior of the material depends essentially on the elastic coefficient k. Moreover, hysteresis loop and the related power exchange,

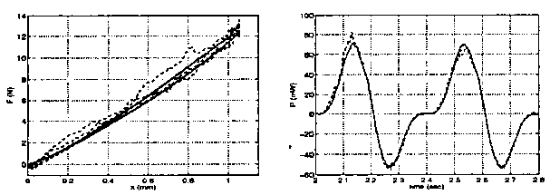

(a) Hysteresis loop (b) Power Exchange

Fig. 6. Hunt-Crossley model: measured (dashed) and estimated (solid) hysteresis loop and power exchange for a thin layer of plastic materials

reported in Fig. 6(b), show good correspondence between the experimental curves and the estimated one. Note that for this class of materials, the Kelvin-Voigt model also provides good estimates, since points A and B of Fig. 1(a) are in this case very close to the origin and therefore a constant damping coefficient does not alter significantly the hysteresis loop.

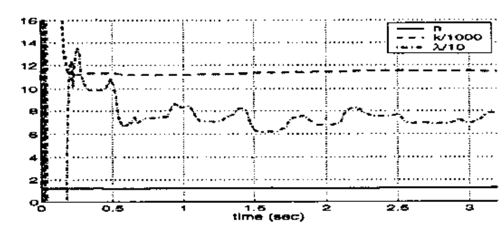

Fig. 7. Hunt-Crossley model: estimation of n (solid), k (dash) and λ (dash-dot) for a thin layer of plastic material

The following values for parameters estimates, see Fig. 7, are obtained: $k \simeq 1.15e4$, $\lambda \simeq 70$, $n \simeq 1.2$. According to what previously discussed about properties of the Hunt-Crossley model, the exponent n, that takes into account geometry of contact surfaces, is about one. We notice that k and n are quite stable around their final value, while λ presents a more oscillatory behavior, because of numerical differentiation used to compute $\dot{x}$ which makes this parameter more sensitive to measurement noise.

C. Soft material

The application of a linear regression algorithm to estimate parameters K and B of the Kelvin-Voigt model for a soft gel provides the results of Fig. 8, with $K \simeq 2.26e3$ N/m and $B \simeq 123$ Ns/m. Drawbacks related to nonzero estimated force when $x = 0$ can be clearly recognized, as well as inconsistencies in power exchange between the probe device and the soft gel.

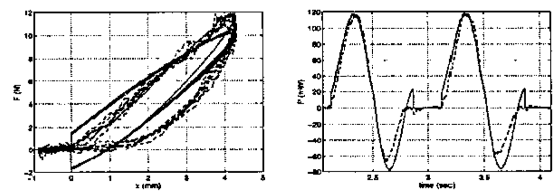

(a) Hysteresis loop (b) Power Exchange

Fig. 8. Linear model: measured (dash) and estimated (solid) hysteresis loop and power exchange for soft gel

On the contrary, hysteresis loop estimated by means of the Hunt-Crossley model is more similar to the measured one (Fig. 9(a)), as well the estimated power exchange, shown in Fig. 9(b), that does not exibit positive "spikes" presents in Fig. 8(b). Only a little discrepancy between the

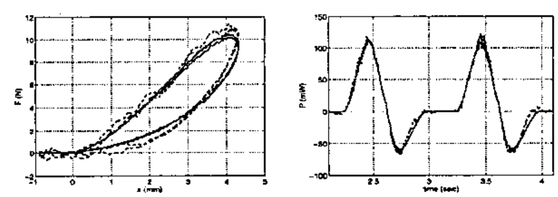

(a) Hysteresis loop (b) Power Exchange

Fig. 9. Hunt-Crossley model: measured (dashed) and estimated (solid) hysteresis loop and power exchange for soft gel

estimated curve and the measured one is present at the end of the restitution phase; this is caused by the fact that the behavior of the soft gel is at the limit of its elasticity region and tends to reveal plastic phenomena.

The convergence of parameters estimates to their final values $k \simeq 1.35e3$, $\lambda \simeq 36$, $n \simeq 1.35$ is shown in Fig. 10 shows. Notice that in this case the value of n is greater than that obtained for the stiff material, since contact surface between the probe device and the soft gel is slightly larger.

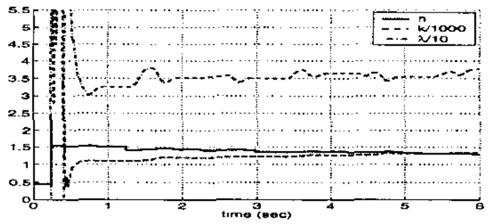

Fig. 10. Hunt-Crossley model: estimation of n (solid), k (dash) and λ (dash-dot) for soft gel

D. Change of material

As mentioned in section III, the use of a forgetting factor allows to improve the detection of material changes. In particular, the case of a switching from the soft gel to the layer of plastic materials has been considered. The hysteresis loop and the power exchange diagram are shown in Fig. 11, which confirm the adequacy of the Hunt-Crossley model to describe both stiff and soft materials. The ability of the estimation algorithm to detect a change in the touched material is shown in Fig. 12. Indeed, after a short transient, the convergence to parameters of the new material is achieved and previous estimates do not affect final values.

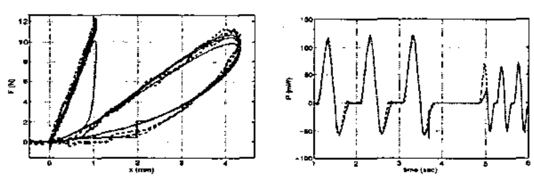

(a) Hysteresis loop (b) Power Exchange

Fig. 11. Hunt-Crossley model: measured (dashed) and estimated (solid) hysteresis loop and power exchange when soft gel is substituted by the thin plastic layer

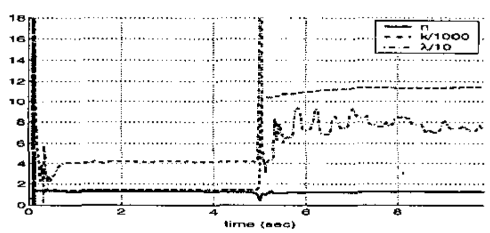

Fig. 12. Hunt-Crossley model: estimation of n (solid), k (dash) and λ (dash-dot) when soft gel is substituted by the thin plastic layer

V. Conclusions and Future Work

The need of accurately represent the contact dynamics between a robotic system and a compliant object requires the choice of a suitable model and of an on-line estimation algorithm. In this paper, the properties of the Hunt-Crossley model have been discussed and compared with those of the traditional linear model. However, the nonlinearity of the former model requires to design an on-line recursive estimator that combines efficiency and good convergence properties. The proposed algorithm has been used to experimentally identify parameters characterizing two different materials. In particular, the advantages of Hunt-Crossley model become clear in the case of the soft gel, where a correct estimate of the hysteresis loop is obtained.

Future work, besides a more formal proof of the convergence of the estimation algorithm, will be aimed at the generalization of the described models and algorithms to the full geometrical contact (6 dof) and to its experimental validation. Moreover, the application of this estimation technique for the improvement of performance of robotic systems interacting with unknown environments will be investigated.

Acknowledgements. This activity has been supported by Geoplex, EU project N. IST-2001-34166. Further information is available at `http://www.geoplex.cc`

References

[1] L. J. Love and W. J. Book, "Environment estimation for enhanced impedance control," in *Proceedings of the IEEE International Conference on Robotics and Automation*, vol. 2, Nagoya, Japan, May 1995, pp. 1854–1859.

[2] N. Hogan, "Impedance control: An approach to manipulation: Part I – Theory, Part II – Implementation, Part III – Applications," *ASME Journal of Dynamic Systems, Measurment and Control*, vol. 107, 1985.

[3] D. Erickson, M. Weber, and I. Sharf, "Contact stiffness and damping estimation for robotic systems," *The International Journal of Robotics Research*, vol. 22, no. 1, pp. 41–57, January 2003.

[4] P. Arcara and C. Melchiorri, *MISTRAL: Methodologies and Integration of Subsystems and Technologies for Anthropic Robots and Locomotion*. Springer-Verlag, 2003, ch. Comparison and Improvement of Control Schemes for Robotic Teleoperation Systems with Time Delay.

[5] E. Colgate, "Robust impedance shaping telemanipulation," *IEEE Transactions on Robotics and Automation*, vol. 9, no. 4, pp. 374–384, August 1993.

[6] S. Hirche and M. Buss, "Passive position controlled telepresence systems with time delay," in *American Control Conference*, vol. 1, Denver, USA, June 2003, pp. 168 – 173.

[7] G. Gilardi and I. Sharf, "Literature survey of contact dynamics modelling," *Journal of Mechanism and Machine Theory*, vol. 37, no. 10, pp. 1213–1239, October 2002.

[8] K. Hunt and F. Crossley, "Coefficient of restitution interpreted as damping in vibroimpact," *ASME Journal of Applied Mechanics*, pp. 440–445, June 1975.

[9] D. W. Marhefka and D. E. Orin, "A compliant contact model with nonlinear damping for simulations of robotic systems," *IEEE Transactions on Systems, Man and Cybernetics - Part A: Systems and Humans*, vol. 29, no. 6, pp. 566–572, November 1999.

[10] S. Stramigioli, "Port-hamiltonian modeling of spatial compliant contacts," in *2nd Workshop on Lagrangian and Hamiltonian Methods for Nonlinear Control (LHMNLC03)*. Sevilla, Spain: IFAC, June 2003.

[11] W. Fluggë, *Viscoelasticity*. Waltham, Mass.: Blaisdell Publishing Company, 1967.

[12] W. Goldsmith, *Impact: The Theory and Physical Behavior of Colliding Solids*. London: Edward Arnold Publishers Ltd, 1960.

[13] K. L. Johnson, *Contact Mechanics*. Cambridge, U.K.: Cambridge Univ. Press, 1989.

[14] L. Ljung and T. Södertström, *Theory and Practice of Recursive Identification*. Cambridge, Massachusetts: The MIT Press, 1983.

[15] Y. Bar-Shalom and X.-R. Li, *Estimation and Tracking: Principles, Techniques, and Software*. Artech House, 1993.